The Astrophysical Journal, 678:614–620, 2008 May 10

THE MOST DARK-MATTER–DOMINATED GALAXIES: PREDICTED GAMMA-RAY SIGNALS FROM THE FAINTEST MILKY WAY DWARFS

Louis E. Strigari,[1] Savvas M. Koushiappas,[2] James S. Bullock,[1] Manoj Kaplinghat,[1]
Joshua D. Simon,[3] Marla Geha,[4] and Beth Willman[5]

Received 2007 October 12; accepted 2008 January 7

ABSTRACT

We use kinematic data from three new nearby, extremely low luminosity Milky Way dwarf galaxies (Ursa Major II, Willman 1, and Coma Berenices) to constrain the properties of their dark matter halos, and from these we make predictions for the γ-ray flux from annihilation of dark matter particles in these halos. We show that these $\sim 10^3\ L_\odot$ dwarfs are the most dark-matter–dominated galaxies known, with total masses within 100 pc that are in excess of $10^6\ M_\odot$. Coupled with their relative proximity, their large masses imply that they should have mean γ-ray fluxes that are comparable to or greater than those of any other known satellite galaxy of the Milky Way. Our results are robust to both variations of the inner slope of the density profile and the effect of tidal interactions. The fluxes could be boosted by up to 2 orders of magnitude if we include the density enhancements caused by surviving dark matter substructure.

Subject headings: cosmology: theory — dark matter

Online material: color figures

1. INTRODUCTION

The census of the Local Group has changed dramatically in the last few years. Prior to the turn of the century, there were only 11 known satellite galaxies of the Milky Way (MW), with a discovery rate of roughly one new Local Group satellite per decade (Mateo 1998). However, the Sloan Digital Sky Survey (SDSS) has been able to uncover a population of extremely low luminosity satellite galaxies, which has roughly doubled the number of known satellites (Willman et al. 2005; Zucker et al. 2006; Belokurov et al. 2007; Irwin et al. 2007; Walsh et al. 2007). Determining how these new satellites fit in a given model for dark matter and cosmology presents a very exciting theoretical challenge.

The cold dark matter (CDM) model predicts the existence of hundreds of MW satellites that are expected to host galaxies at the faint end of the luminosity function (Kauffmann et al. 1993; Klypin et al. 1999; Moore et al. 1999). The ability of gas to cool and form stars in these low-mass dark matter halos depends on a number of complex physical processes, such as supernova feedback, the photoionizing background, and mass loss due to tidal interactions (Dekel & Silk 1986; Cole et al. 1994; Somerville & Primack 1999; Barkana & Loeb 1999; Bullock et al. 2000; Chiu et al. 2001; Benson et al. 2002). Despite the broad range of observed luminosities, the dark matter masses for all of the pre-SDSS satellites are constrained to within a relatively narrow range, approximately $\sim 1\text{–}6 \times 10^7\ M_\odot$ within their inner 600 pc (Walker et al. 2007; Strigari et al. 2007a). Understanding this strong luminosity bias at the low-mass end is crucial to deciphering the formation of these dwarf spheroidal (dSph) galaxies, as well as to constraining the nature of dark matter.

In this paper we show that three new and nearby members of the Local Group discovered by the SDSS (Willman 1, Coma Berenices, and Ursa Major II) are likely to have masses that are comparable to those of their more luminous counterparts. Initial estimates have already shown that these galaxies have mass-to-light ratios that are similar to or larger than those of the pre-SDSS dwarfs (Martin et al. 2007; Simon & Geha 2007). With luminosities that are more than 2 orders of magnitude less than those of the pre-SDSS dwarfs, these new satellites are interesting not only in the context of galaxy formation at the lowest mass scales, but also for indirect dark matter detection. The new dwarfs are very faint, but they contain large amounts of dark matter and are located quite nearby, which makes them ideal sites to search for signals of dark matter annihilation.

Current and future observatories, including space-based experiments, such as *GLAST* (Ritz et al. 2006), as well as a suite of ground-based Cerenkov detectors, such as STACEE (Hanna et al. 2002), H.E.S.S. (Hofmann 2003), MAGIC (Cortina 2005), VERITAS (Weekes et al. 2002), CANGAROO (Yoshikoshi et al. 1999), and HAWK (Sinnis 2005), will search for the signal of γ-rays from dark matter annihilations. The prospects for γ-ray detection from dark matter in well-known MW satellites with these observatories has been the subject of many previous studies (Baltz et al. 2000; Evans et al. 2004; Profumo & Kamionkowski 2006; Bergstrom & Hooper 2006; Strigari et al. 2007b; Sánchez-Conde et al. 2007). All of these systems are interesting targets not only because of their large mass-to-light ratios, but also because they are expected to have very low intrinsic γ-ray emission. This is in contrast to the situation at the Galactic center, where astrophysical backgrounds hinder the prospects of extracting the signal from dark matter annihilation (Hooper & Dingus 2004). Moreover, the known location of the MW satellites makes a search of dark matter annihilation well-defined, unlike the search of completely dark substructure, which would rely on serendipitous discovery (Calcaneo-Roldan & Moore 2000; Tasitsiomi & Olinto 2002; Stoehr et al. 2003; Koushiappas et al. 2004; Pieri et al. 2005; Koushiappas 2006; Diemand et al. 2007; Baltz et al. 2007).

From the mass modeling of the dark matter halos, we provide the first determination of the γ-ray signal from dark matter from Ursa Major II, Willman 1, and Coma Berenices ("Coma" hereafter). These galaxies provide promising targets for γ-ray detection for three reasons: (1) they are the among the closest

[1] Center for Cosmology, Department of Physics and Astronomy, University of California, Irvine, CA 92697.
[2] Theoretical Division and ISR Division, Los Alamos National Laboratory, Los Alamos, NM 87545.
[3] Department of Astronomy, California Institute of Technology, Pasadena, CA 91125.
[4] National Research Council of Canada, Herzberg Institute of Astrophysics, Victoria, BC V9E 2E7, Canada.
[5] Harvard-Smithsonian Center for Astrophysics, Cambridge, MA 02138.

TABLE 1
PROPERTIES OF MILKY WAY SATELLITES

Galaxy	Distance (kpc)	Luminosity ($10^3\ L_\odot$)	Core Radius (kpc)	Cutoff Radius (kpc)	Number of Stars
Ursa Major II	32	2.8	0.127 (P)	...	20
Coma Berenices	44	2.6	0.064 (P)	...	59
Willman 1	38	0.9	0.02 (K)	0.08 (K)	47
Ursa Minor	66	290	0.30 (K)	1.50 (K)	187

NOTES.—The distance, luminosity, and core and cutoff radii [Plummer (P) or King (K)] for each of the Milky Way satellites that we study. The last column gives the total number of stars used in the analysis.

dark-matter–dominated systems, (2) they are expected to be free from intrinsic γ-ray emission, and (3) present data on their stellar kinematics suggest that their dark matter halos are as massive as those of the more well-known population of MW satellites.

This paper is organized as follows. In § 2, we review the theoretical modeling of dwarf dark matter halos and the calculation of the γ-ray flux. In § 3, we present the likelihood function for determining the flux and outline the theoretical priors in the modeling. In §§ 4 and 5 we present the results and the discussion.

2. THEORETICAL MODELING

When modeling the stellar distribution of a dwarf galaxy, it is important to determine the effect of external tidal forces on the dynamics of the system. For the MW satellites we study, we can obtain an estimate of the external tidal force by comparing its magnitude to the internal gravitational force. The internal gravitational force is $\sim\sigma^2/R$, and the external tidal force from the MW potential is $\sim(220\ \mathrm{km\ s^{-1}})^2 R/D^2$, where D is the distance to the dwarf from the center of the MW and 220 km s^{-1} is the MW rotation speed at the distance of the dwarf. The MW satellites are characterized by scale radii of $R \sim 10$–100 pc and velocity dispersions of $\sigma \sim 5$–10 km s^{-1}. For a typical distance of $D \sim 40$ kpc, the internal gravitational forces are thus larger by factors of $\sim$100.

An additional estimate of tidal effects can be obtained by comparing the internal crossing times of the stars in the galaxy to the orbital timescale of the system in the external potential of the host. For a galaxy with scale radii and velocity dispersions as given above, an estimate of the crossing time is given by $R/\sigma \sim 1$–20 Myr. If we assume a rotation speed of $\sim$220 km s^{-1} at the distance of these satellites ($\sim$40 kpc), their orbital timescale in the MW potential is $\sim$Gyr.

From the above estimates we conclude that it is *highly unlikely* that these galaxies are presently undergoing significant tidal stripping. These galaxies may have been tidally stripped before (for example, if their orbit took them closer to the center of the MW); however, the stellar core that has survived is faithfully tracing the local potential (Piatek & Pryor 1995; Klimentowski et al. 2007; Peñarrubia et al. 2008). Of the galaxies that we consider, only Ursa Major II shows strong evidence of past tidal interaction, as it is located on the same great circle as the Orphan Stream discovered by the SDSS (Zucker et al. 2006; Belokurov et al. 2007). Thus, we can proceed ahead with confidence in modeling the surviving stellar cores as systems in dynamical equilibrium.

Line-of-sight velocities are widely used to determine the properties of the dark matter halos of dSphs (Łokas et al. 2005; Mashchenko et al. 2006; Gilmore et al. 2007), under the assumption of spherical symmetry. For a system in dynamical equilibrium, the spherically symmetric Jeans equation gives the stellar line-of-sight velocity dispersion at a projected radius, R, from the center of the galaxy as

$$\sigma_t^2(R) = \frac{2}{I(R)} \int_R^\infty \left(1 - \beta \frac{R^2}{r^2}\right) \frac{\rho_\star \sigma_r^2 r}{\sqrt{r^2 - R^2}}\, dr, \qquad (1)$$

where the three-dimensional velocity dispersion, σ_r, is obtained from

$$r \frac{d(\rho_\star \sigma_r^2)}{dr} = -\rho_\star(r) V_c^2(r) - 2\beta(r)\rho_\star \sigma_r^2. \qquad (2)$$

Here β is the stellar velocity anisotropy and $\rho_\star(r)$ is the density profile for the stellar distribution, which is obtained from the projected stellar distribution, $I(R)$. The stellar distributions of the dSphs are typically fitted with either Plummer or King profiles (King 1962). The primary difference between these fits is that Plummer profiles are described by a single parameter, $r_{\rm P}$, and fall off as a power law in the outer regions of the galaxy, whereas King profiles are described by a core radius, $r_{\rm K}$, and a cutoff radius, $r_{\rm cut}$, and fall off exponentially in the outer regions. For the stellar distributions of Ursa Major II and Coma, we use the Plummer fits compiled in Simon & Geha (2007), and for Willman 1 we use the King profile fit from Martin et al. (2007). These quantities, along with the distance to each galaxy and their respective luminosities, are given in Table 1.

We model the distribution of dark matter in the Milky Way satellites with radial density profiles of the form

$$\rho(r) = \frac{\rho_s}{\tilde{r}^\gamma (1 + \tilde{r})^{3-\gamma}}, \qquad (3)$$

where ρ_s is the characteristic density, $\tilde{r} = r/r_s$, and r_s is the scale radius. Numerical simulations bound the values of γ in the range [0.7, 1.2], and the outer slope is approximately -3 (Navarro et al. 2004; Diemand et al. 2005). In order to compare the mass distribution in the satellites to those of dark matter halos in N-body simulations, it is useful to work in terms of the two parameters $V_{\rm max}$ and $r_{\rm max}$, which are the maximum circular velocity and the radius at which it is obtained. For example, for $\gamma = (0.8,\ 1,\ 1.2)$, $r_{\rm max}/r_s = (2.61,\ 2.16,\ 1.72)$. Thus, for a particular value of γ, the density profiles of dark matter halos can be described by either the ρ_s-r_s relation or, similarly, by the $V_{\rm max}$-$r_{\rm max}$ relation.

With the parameters of the halo density profile specified, the γ-ray flux from dark matter annihilations is given by

$$\Phi = \frac{1}{2} P \int_0^{\xi_{\rm max}} \sin\xi\, d\xi \int_{\eta_-}^{\eta_+} \left[\frac{\rho_s}{\tilde{r}^\gamma (1 + \tilde{r})^{3-\gamma}}\right]^2 d\eta, \qquad (4)$$

where $\eta_{\pm} = D\cos\xi \pm (r_t^2 - D^2\sin^2\xi)^{1/2}$, D is the distance to the galaxy, ξ is the angular distance from the center of the galaxy, and r_t is the tidal radius for the dark matter halo. Note that in the limit of $D \gg r_s$, the flux scales as $\int \rho(r)^2\, dr/D^2$, and in the particular case in which $\gamma = 1$, $\Phi \sim \rho_s^2 r_s^3/D^2$, with $\sim$90% of the flux originating within r_s.

In equation (4), the properties of the dark matter particle are determined by

$$P = \frac{\langle\sigma v\rangle}{M_x^2}\int_{E_{\rm th}}^{M_\chi}\frac{dN}{dE}\,dE. \quad (5)$$

Here $E_{\rm th}$ is a threshold energy, M_χ is the mass of the dark matter particle, $\langle\sigma v\rangle$ is the annihilation cross section, and the spectrum of the emitted γ-rays is given by dN/dE. Unless otherwise noted, we assume that $P \approx 10^{-28}$ cm^3 s^{-2} GeV^{-2}, which corresponds to the most optimistic supersymmetric dark matter models. However, we stress that the derived results can be rescaled to any dark matter model by a simple rescaling of P.

3. LIKELIHOOD FUNCTION AND PRIORS

Observed stellar line-of-sight velocities place strong constraints on several important parameters that describe the dark matter halos of dSphs. Two examples of these parameters are the halo mass and density at a characteristic halo radius, corresponding to about twice the King core radius (or about 600 pc for a typical dSph; Walker et al. 2007; Strigari et al. 2007a). More relevant to γ-rays is the quantity $\rho_s^2 r_s^3$ (the γ-ray luminosity is $\sim\rho_s^2 r_s^3$), which is typically determined to within a factor of 3–6 with the line-of-sight velocities of several hundred stars (Bergstrom & Hooper 2006; Strigari et al. 2007b). The constraints on these parameters can be strengthened by including relations between similar parameters observed in numerical simulations. When combined with the observational constraints, these empirical relations in numerical simulations constitute a theoretical prior, delineating a preferred region of the parameter space of the dark matter distribution in dSphs (Strigari et al. 2007b; Peñarrubia et al. 2007). In this section, we discuss the implementation of this prior and derive the general form of the likelihood function that we use to constrain the γ-ray flux from dark matter annihilations.

We assume that the line-of-sight velocities are drawn from a Gaussian distribution centered on the true value of the mean velocity, u. This has been shown to be a good description of the well-studied dwarfs with line-of-sight velocities from several hundred stars (Walker et al. 2006). Given the set of theoretical parameters, the probability to obtain the set of observed line-of-sight velocities, $\boldsymbol{x}$, is

$$P(\boldsymbol{x}|\boldsymbol{\theta}) = \prod_{i=1}^{n}\frac{1}{\sqrt{2\pi(\sigma_{t,i}^2+\sigma_{m,i}^2)}}\exp\left[-\frac{1}{2}\frac{(v_i-u)^2}{\sigma_{t,i}^2+\sigma_{m,i}^2}\right]. \quad (6)$$

Here $\boldsymbol{\theta}$ is the set of parameters that describe the dSph, and the sum is over the observed total number of stars. The dispersion in the velocities thus has two sources: (1) the intrinsic dispersion, $\sigma_{t,i}(\boldsymbol{\theta})$, which is a function of the position of the ith star, and (2) the uncertainty stemming from the measurement, $\sigma_{m,i}$.

We can simplify equation (6) by assuming that the measurement uncertainties are small relative to the intrinsic dispersion. This is a good approximation for well-studied dwarfs, which have intrinsic dispersions of $\sim$10 km s^{-1} and measurement errors of $\sim$1 km s^{-1} (Westfall et al. 2006; Koch et al. 2007). Under this approximation, equation (6) becomes

$$P(\boldsymbol{x}|\boldsymbol{\theta}) = \prod_{i=1}^{N_b}\frac{1}{\sqrt{2\pi\sigma_{t,i}^2}}\exp\left(-\frac{1}{2}\frac{N_i\hat{\sigma}_{t,i}^2}{\sigma_{t,i}^2}\right), \quad (7)$$

where the sum is now over the number of bins, N_b, for which the velocity dispersion is determined. The velocity dispersion in the ith bin is $\hat{\sigma}_{t,i}^2$, and the number of stars in the ith bin is N_i. We can use equation (7) if the observations are given by line-of-sight velocity dispersions and if the measurement errors are small in comparison to the intrinsic dispersion. This is the case for Ursa Minor, as is discussed below.

We describe the dark matter halos in terms of the parameter $\boldsymbol{\theta} = (V_{\rm max},\, r_{\rm max},\, \beta)$. We assume that β is constant as a function of radius and let it vary over the range $[-5, 1]$. We integrate equations (6) and (7) over these parameters and define the likelihood function for a fixed γ-ray flux, f, as

$$\mathcal{L}(f) \propto \int P(\boldsymbol{x}|V_{\rm max},\, r_{\rm max},\, \beta)P(V_{\rm max},\, r_{\rm max}) \times \delta(\Phi(V_{\rm max},\, r_{\rm max}) - f)\, dV_{\rm max}\, dr_{\rm max}\, d\beta. \quad (8)$$

Here we have assumed a uniform prior on β, and the prior probability distribution for $V_{\rm max}$ and $r_{\rm max}$ is given by $P(V_{\rm max},\, r_{\rm max})$. This prior distribution is determined by the $V_{\rm max}$-$r_{\rm max}$ relation from CDM simulations.

In order to determine $P(V_{\rm max},\, r_{\rm max})$, we need both its mean relation and its halo-to-halo scatter. For dark subhalos that have been strongly affected by tidal interactions, the $V_{\rm max}$-$r_{\rm max}$ relation is strongly dependent on the nature of the potential of the host system, as these systems undergo varying amounts of mass loss as they evolve within the host halo. For example, Bullock & Johnston (2007) have embedded a disk potential in a MW-size host halo, and they found that the $V_{\rm max}$-$r_{\rm max}$ relation of subhalos takes the form $\log(r_{\rm max}) = 1.35[\log(V_{\rm max}) - 1] - 0.196$. We obtain a similar slope by examining the subhalos in the dark-matter–only Via Lactea simulation of MW substructure (Diemand et al. 2007); however, differences in the assumed cosmological parameters, as well as the absence of a disk potential in Via Lactea, translate into differences in the normalization of the $V_{\rm max}$-$r_{\rm max}$ relation. For Via Lactea subhalos, we find that the normalization is reduced by $\sim$30%, which implies reduced halo concentrations (larger values of $r_{\rm max}$ for fixed values of $V_{\rm max}$).

We model the scatter in $V_{\rm max}$ as a lognormal distribution, with $\sigma_{\log V_{\rm max}} \simeq 0.20$. This provides a conservative estimate for the scatter in $V_{\rm max}$ as a function of $r_{\rm max}$ for nearly the entire range of the subhalo mass function. At the extremely high end of the subhalo mass function ($V_{\rm max} \gtrsim 20$ km s^{-1}), the scatter increases because in this range it is dominated by a small number of very massive systems that have been accreted into the host halo very recently. This increase in the scatter is simply because Via Lactea is only one realization of a substructure population in a MW halo. We find that by excluding the extreme outliers in the Via Lactea mass function, the scatter is similar to that of the low-mass regime. This is a similar result to those obtained in semianalytic

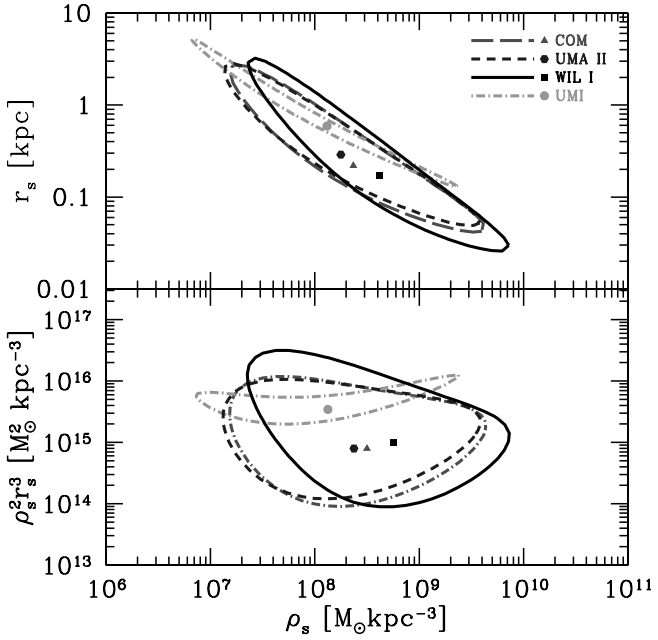

FIG. 1.—90% confidence level regions in the r_s-ρ_s (*top*) and $\rho_s^2 r_s^3$-ρ_s (*bottom*) parameter spaces for Coma, Ursa Major II, Willman 1, and Ursa Minor. We marginalize over the velocity anisotropy and have assumed an inner slope of $\gamma = 1$. The best-fit values are indicated with symbols. [*See the electronic edition of the Journal for a color version of this figure.*]

models of many realizations of the subhalo population (Zentner & Bullock 2003; van den Bosch et al. 2005).

4. RESULTS

4.1. *Flux Estimates for Smooth Dark Matter Distributions*

We now quantify the prospects for detecting γ-rays from dark matter annihilation in the three new satellite galaxies. We first assume that the dark matter is distributed smoothly, and we discuss the implications of a boost factor due to substructure in the next subsection. We use observations of these galaxies from the following references: Simon & Geha (2007) for Ursa Major II and Coma, and B. Willman et al. (2008, in preparation) for Willman 1. For these galaxies we have individual stellar velocities, so we use the likelihood function in equation (6). For Willman 1, from our sample of 47 stars we determine a central velocity dispersion of $\sim 4.8 \pm 0.9$ km s^{-1}, which is in agreement with the 11 star sample of Martin et al. (2007). However, since our sample contains a much larger number of member stars, we prefer to use our sample for consistency. To make a connection to previous studies of dark matter annihilation in Milky Way satellites, we compare the fluxes for these new satellites to the flux from Ursa Minor, which is at a distance of $D = 66$ kpc and has a luminosity of $L = 2.9 \times 10^5\, L_\odot$. Ursa Minor has the largest flux of any of the well-known dwarfs (Strigari et al. 2007b). We describe the stellar distribution of Ursa Minor with a King profile, with $r_K = 0.30$ kpc and $r_{cut} = 1.50$ kpc (Muñoz et al. 2005). For Ursa Minor we use the measured velocity dispersion from a sample of 187 stars distributed evenly in 11 bins (Muñoz et al. 2005), and we use the likelihood function given in equation (7).

In the top panel of Figure 1, we show the 90% confidence level (c.l.) region in the r_s-ρ_s plane for each galaxy, where the best-fit values are denoted by symbols. Here we use the V_{max}-r_{max} prior from § 3, and we take the inner slope of the dark matter halo profile to be $\gamma = 1$. In the bottom panel of Figure 1 we show the 90% confidence level region in the $\rho_s^2 r_s^3$-ρ_s plane. As seen in Figure 1, the range of values that $\rho_s^2 r_s^3$ can take in each satellite is reduced with the inclusion of more stars (e.g., Ursa Minor vs. any one of the other three satellites).

TABLE 2
MASSES AND MAXIMUM CIRCULAR VELOCITIES FOR MILKY WAY SATELLITES

Galaxy	Mass at <100 pc ($10^6\, M_\odot$)	V_{max} (km s^{-1})
Ursa Major II	$3.1^{+5.6}_{-1.8}$	23^{+69}_{-10}
Coma Berenices	$1.9^{+2.1}_{-1.0}$	19^{+53}_{-9}
Willman 1	$1.3^{+1.5}_{-0.8}$	27_{-15}
Ursa Minor	$2.3^{+1.9}_{-1.2}$	30^{+12}_{-16}

NOTES.—Masses within 100 pc and maximum circular velocities of the Milky Way satellites we study. Errors indicate the 90% c.l. regions. No upper limit could be obtained for the maximum circular velocity of Willman 1.

The constrained regions in Figure 1 can be used to determine the masses, maximum circular velocities, and γ-ray flux probability distributions for each galaxy. In Table 2, we show the masses within 100 pc and the maximum circular velocities for each galaxy. The errors indicate the 90% c.l. regions.

To determine the flux distributions, we must first specify a solid angle for integration. For optimal detection scenarios, the solid angle should encompass the region with the largest signal-to-noise ratio. For the present work, we will integrate over the region in which 90% of the flux originates. As discussed above, for the particular case in which $\gamma = 1$, 90% of the flux originates within r_s. Therefore, in order to estimate the solid angle of integration, we have to first determine the maximum likelihood values of r_s. This is done by marginalizing over ρ_s and β with the V_{max}-r_{max} prior. The distributions of angular sizes are then obtained from $\mu = \tan^{-1}(r_s/D)$, where D is the distance to the satellite. As is shown in Figure 2, we find that, given their similar size and roughly similar distances, all three satellites will emit 90% of their γ-ray flux within a region of $\sim 0.2^\circ$, centered on each satellite (for $\gamma = 1$).

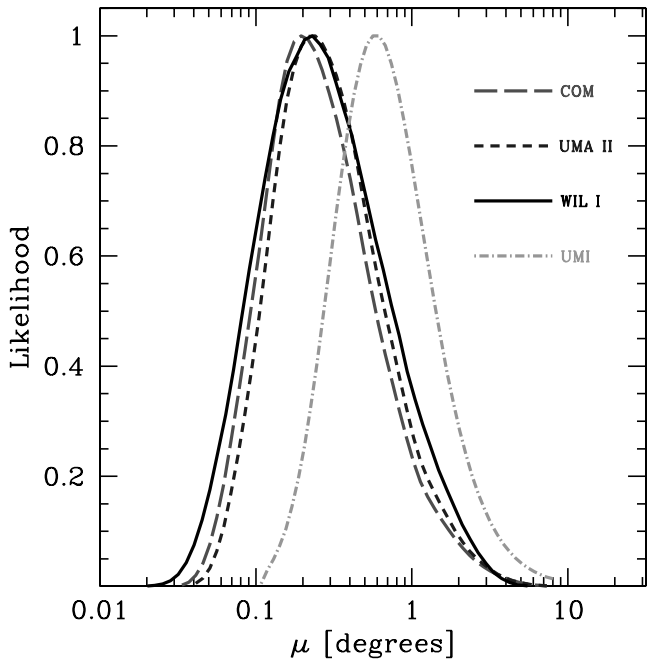

FIG. 2.—Probability distributions of the angular size subtended by r_s for each galaxy. We marginalize over the velocity anisotropy and ρ_s. The inner slope is fixed to $\gamma = 1$. [*See the electronic edition of the Journal for a color version of this figure.*]

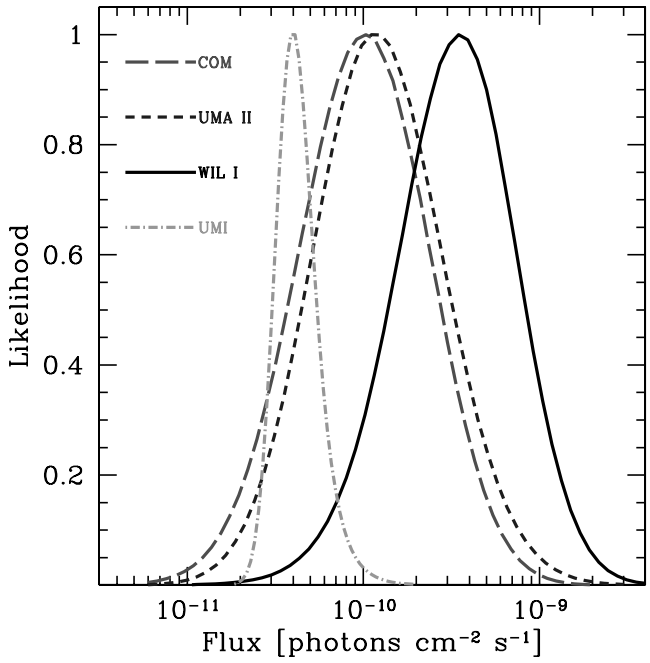

FIG. 3.—Probability distributions for the γ-ray fluxes from Coma, Ursa Major II, Willman 1, and Ursa Minor, where we have marginalized over the velocity anisotropy, ρ_s, and r_s. We assume a value of $P = 10^{-28}$ cm^3 s^{-1} GeV^{-2} and an inner slope of $\gamma = 1.0$. We have assumed no boost from halo substructure, which increases these fluxes by a factor of $\sim$10–100. [*See the electronic edition of the Journal for a color version of this figure.*]

Ursa Minor is the most physically extended galaxy, subtending the largest projected area on the sky.

It is important to determine whether each of the galaxies will be detected as point sources, or whether they will be resolved as extended objects. To determine this we compare their angular size to the angular resolution of γ-ray telescopes. *GLAST* will have a single-photon angular resolution of $\sim 10'$ for energies greater than 1 GeV, similar to the angular resolution of ground-based detectors (such as VERITAS) for energies greater than a few tens of GeV. In the case in which the detected number of photons is $N_\gamma > 1$, the angular resolution of a detector is improved by a factor of $1/(N_\gamma)^{1/2}$. Therefore, these galaxies can be resolved as extended objects, which in principle would allow a measured flux to determine the distribution of dark matter in the halo itself.

Figure 3 depicts the resulting flux probability distribution for the three new satellites and Ursa Minor. These are obtained by marginalizing over β, ρ_s, and r_s and including the $V_{\rm max}$-$r_{\rm max}$ prior. We set the inner slope to $\gamma = 1$ and integrate the flux over the solid angle that corresponds to 0.2° from the center of the galaxy. We assume a value of $P = P_0 = 10^{-28}$ cm^3 s^{-1} GeV^{-2}, but the result can be scaled to any dark matter candidate with a different value of P by simply multiplying the flux distribution by a factor of P/P_0.

The relative proximity of the three new satellites, and their comparable sizes, results in γ-ray fluxes that are roughly similar. For $P \approx P_0$, the likelihood peaks at approximately $\Phi_0 \approx 10^{-10}$ cm^{-2} s^{-1}, with a spread of nearly an order of magnitude. Thus, Ursa Major II, Coma, and Ursa Minor all have comparable fluxes, and Willman 1 has a most likely flux that is about 3 times larger than those of Ursa Major II or Coma.

4.2. *The Effects of the Inner Slope and Substructure Boost Factors*

Understanding the distribution of dark matter in the inner regions of the galaxies also has important implications for detecting a γ-ray flux. However, when varying the inner slope, we must also be certain to vary all of the other halo parameters so as to remain consistent with the line-of-sight observations. In order to quantify the effects of varying the inner slope, we marginalize over $V_{\rm max}$, $r_{\rm max}$, and β for profiles with different values of γ. In Figure 4 we show the effects of varying the value of γ for Coma and Ursa Minor. The shifts in the flux distribution function are not only a result of varying the inner slope, but also come from the constraints imposed by the data on the density profile parameters ρ_s and r_s. The relative amount of the shifts can be understood by considering the best-fitting values of r_s (where the majority of the γ-ray flux comes from) as compared to the core radii of the systems. When the core radius is similar to r_s, the shifts are larger for varying values of γ, as in the case of Ursa Minor. However,

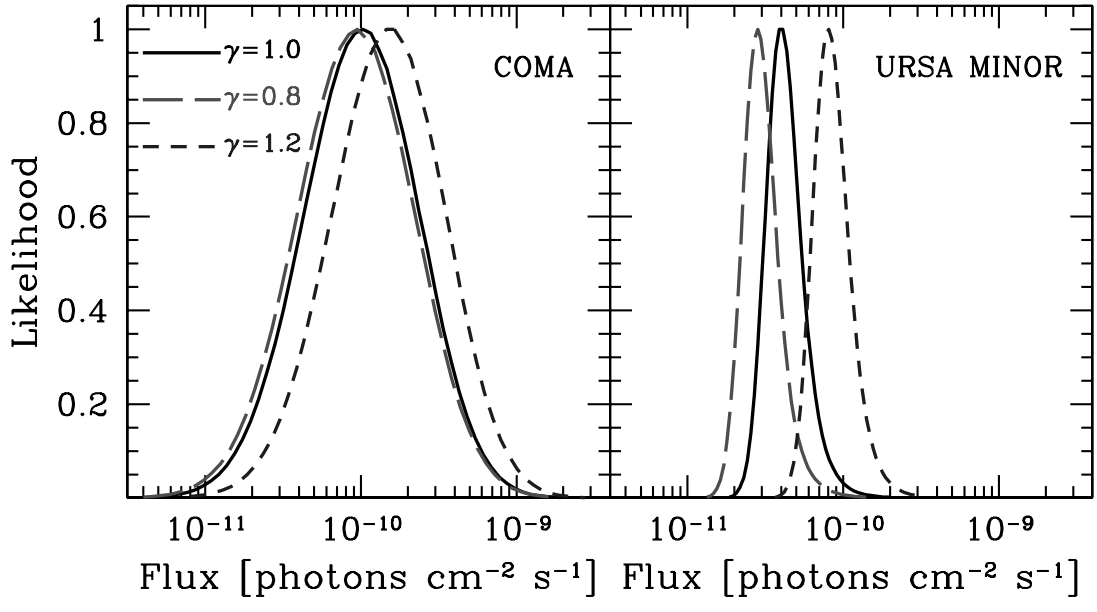

FIG. 4.—Probability distributions for the γ-ray flux of Coma and Ursa Minor for inner slopes of 0.8 (*long-dashed lines*), 1.0 (*solid lines*), and 1.2 (*short-dashed lines*). We marginalize over the same quantities as in Fig. 3. The value of P is the same as in Fig. 3. [*See the electronic edition of the Journal for a color version of this figure.*]

when the core radius is much smaller than the fitted values of r_s, variations in the inner slope are less significant than the change induced by ρ_s, as is the case for Coma.

The presence of substructure in dark matter halos is firmly established on theoretical and numerical grounds. Dark matter halos are approximately self-similar, and substructure is expected to be present in all dark matter halos with masses greater than the cutoff scale in the primordial power spectrum, set by the kinetic decoupling temperature of the dark matter particle (for detecting the smallest dark matter halos in the Milky Way, see Koushiappas 2006). It is therefore natural to expect that these galaxies contain substructure if they consist of CDM.

The density enhancement over the smooth distribution of dark matter leads to an enhancement in the total annihilation rate, typically quantified in terms of a "boost" factor. As was shown in Strigari et al. (2007b), the boost factor cannot attain arbitrarily large values, but instead is bounded to be less than $\sim$100, with the exact value depending on the cutoff scale in the CDM mass function. The boost is a multiplicative quantity, so the effect of dark substructure is simply accounted for by scaling the fluxes in Figure 3 by the appropriate boost factor.

4.3. *Detection Prospects*

As is shown in Figure 3, the flux probability distribution functions peak around $\Phi_0 \approx 10^{-10}$ cm^{-2} s^{-1} without including any enhancement to the signal from substructure. Here we assume a conservative value of 10 for the boost factor and discuss the prospects for detecting the three new satellites with γ-ray instruments. We can make simple estimates for the likelihood for detection by adopting the specifications of particular γ-ray detectors. We will use two examples: a space-based experiment, *GLAST*, and a ground-based Cerenkov telescope, VERITAS. For *GLAST*, if we assume an orbit-averaged effective area of $A_{\rm eff} \approx 2 \times 10^3$ cm^2 and an exposure time of $t_{\rm exp} = 10$ yr, their product is $B_G = A_{\rm eff} t_{\rm exp} \approx 3 \times 10^{11}$ cm^2 s. A 50 hr exposure with VERITAS ($A_{\rm eff} \approx 10^8$ cm^2) has $B_V \approx 2 \times 10^{13}$ cm^2 s. Naively, for a fixed value of P, a ground-based detector seems more sensitive because $B_V > B_G$. However, the backgrounds for a ground-based detector are also larger and include a component from the hadronization of cosmic rays in the atmosphere.

As an example, for a fixed value of $P = P_0$ and a solid angle that corresponds to an angular size of 0.2°, the number of photons detected by *GLAST* is $N_{\gamma,G} \approx 300$. The dominant source of background for *GLAST* is the Galactic diffuse emission [$dN_B/dE = 1.2 \times 10^{-6} (E_{\rm th}/{\rm GeV})^{-1.1}$ cm^{-2} s^{-1} sr^{-1} GeV^{-1}; Hunter et al. 1997]. If we assume an energy threshold of $E_{\rm th} \approx 1$ GeV, then the number of background photons is $N_B = B_G dN_B/dE \approx 250$, which means that the new satellites will be detected at approximately a $N_{\gamma,G}/(N_B + N_{\gamma,G})^{1/2} \approx 12\ \sigma$ level. A similar estimate can be obtained for VERITAS. The number of photons detected above 50 GeV in an instrument with an effective area times exposure of $\sim B_V$ is $N_\gamma \approx 2 \times 10^4$. The dominant contribution to the background are photons that originate from neutral pion decays from the nuclear interactions of cosmic rays in the upper layers of the atmosphere [$dN_B/dE = 3.8 \times 10^{-3} (E_{\rm th}/{\rm GeV})^{-2.75}$ cm^{-2} s^{-1} sr^{-1} GeV^{-1}; Nishimura et al. 1980]. The number of background photons from pion decays is approximately $N_B \approx 2 \times 10^7$, and therefore the three satellites could be detected at a $\nu \approx 5\ \sigma$ level. Understanding and discriminating against the background contamination in Cerenkov telescopes is very important in improving the prospects for detecting satellites of the Milky Way.

As is shown in Strigari et al. (2007b), the large number of stellar velocities obtained in the older dSphs allow useful γ-ray flux ratios between different dSphs to be determined. For the three new satellites considered in this work, the kinematic data are not good enough to play the same game. Clearly, more stellar velocities will shrink the allowed region of the $\rho_s^2 r_s^3$ parameter, permitting us to make robust estimates of flux ratios between the galaxies studied here and the rest of the Milky Way satellites.

5. DISCUSSION AND CONCLUSIONS

In this paper, we have modeled the dark matter distribution in three recently discovered Milky Way (MW) satellites (Ursa Major II, Willman 1, and Coma Berenices) and have presented the prospects for detecting γ-rays from dark matter annihilations in their halos. We show that the expected flux from these galaxies is larger than the flux from any of the higher luminosity, more well known (pre-SDSS) dwarfs. There are two reasons for this surprising result: (1) the masses of these new dwarfs within their stellar distributions are similar to the masses of the well-known, larger luminosity dwarfs, and (2) all three new galaxies are closer than the other well-known dwarfs. The implied mass-to-light ratios, $\sim$1000, of these new dwarfs make them the most dark-matter–dominated galaxies known.

Our estimates show that it is unlikely that the observed stellar distributions are presently undergoing tidal disruption. However, this does not mean that they have been free from tidal interactions in the past, but rather that the surviving stellar core can be faithfully modeled as a system in dynamical equilibrium. By including the $V_{\rm max}$-$r_{\rm max}$ CDM prior, we have naturally accounted for tidal effects in the mass modeling, since this $V_{\rm max}$-$r_{\rm max}$ relation in fact comes from dark matter halos that have experienced tidal stripping.

One of the galaxies that we consider, Ursa Major II, may be a candidate for past tidal disruption, given that it is positioned on the same great circle as the Orphan Stream of stars, which was also recently detected by the SDSS (Zucker et al. 2006; Belokurov et al. 2007). This is consistent with the findings of Simon & Geha (2007), who have recently investigated the possibility of tidal disruption in Ursa Major II, as well as all of the other new dwarfs, using proxies such as gradients in the observed velocity distribution and metallicity of the stellar populations. Given the total mass-to-light ratio that we have determined for Ursa Major II, tidal stripping will have only been significant if its pericenter is $\sim$3 times closer than its present distance. Future observations of the stellar distributions in Ursa Major II, and all of the other new faint dwarfs, will be important in determining bound and unbound stellar populations. With a larger sample of stars from a galaxy such as Ursa Major II, it will be possible to remove unbound and interloping stars with techniques similar to those presented in Piatek & Pryor (1995) and Klimentowski et al. (2007). Upon removal of stars unbound to the galaxy, these authors show that in most cases the true bound mass of the system can be recovered to typically better than 25%.

As a very conservative check for the effects of membership uncertainties, we have redone the analysis for each of the galaxies by just keeping the stars within the inner half of each galaxy, where the surface densities are the most well determined. We find that the peak of the flux likelihood is shifted by a small amount relative to the 1 σ widths in Figure 3. Note, however, that even when including the entire population of stars in the observed samples, in all cases equilibrium models provide adequate descriptions of the dynamics of each system.

Unresolved binary star systems also introduce a systematic that may affect the fluxes we have presented. Olszewski et al. (1996) have determined the effect of binaries on the velocity dispersion

of two of the most luminous dwarfs, Draco and Ursa Minor, by inferring the binary population of these systems using multiple-epoch observations. They find a velocity dispersion of ~ 1.5 km s^{-1} due to binaries and a probability of 5% that binaries elevate the velocity dispersion to 4 km s^{-1}, which is still less than the velocity dispersion of the three new dwarfs. Thus, if Ursa Major II, Willman 1, and Coma have binary fractions that are similar to those of Draco and Ursa Minor, their observed velocity dispersions are not significantly affected by binaries. We note that this is consistent with recent estimates of the binary fraction in low-density Galactic globular clusters (Sollima et al. 2007).

A strong test for the presence of binaries is to examine the distribution of measured velocities. The velocity distribution due to internal motion in binary systems should be flat, due to the observed broadness of the period distribution of binaries (Duquennoy & Mayor 1991). The observed period distributions depend on the spectral type and age of the system (among other variables), but are all broad, with dispersions of about 2 orders of magnitude, which seems to be consistent with theoretical expectations (Fisher 2004). Further, there is no observational evidence or theoretical argument that suggests that the period distribution should be sharply suppressed for all periods below ~ 1000 yr (roughly, velocities larger than ~ 3 km s^{-1}). Thus, if there is a large contribution from internal motion in binary stellar systems to the intrinsic velocity dispersion of these dwarfs, we would expect to see a significant tail of high velocities. This is not observed, and hence we can be confident that the measured velocity dispersion is tracing the total mass in the dwarf galaxy.

The new, ultra–low-luminosity galaxies represent an interesting confluence of astronomical and γ-ray studies. Future kinematic studies of all of these new dwarfs will further reduce the errors on the mass distributions and will sharpen the predictions for γ-ray observatories searching for signatures of dark matter annihilations.

We are grateful to Simon White for many useful discussions on likelihood functions for dwarf galaxies; to Jay Strader and Connie Rockosi for Willman 1 data; to Juerg Diemand, Michael Kuhlen, and Piero Madau for making the data from the Via Lactea simulation publicly available; and to John Beacom, Nicolas Martin, and Joe Wolf for useful discussions. J. S. B., L. E. S., and M. K. are supported in part by NSF grant AST-0607746. Work at LANL was carried out under the auspices of the NNSA of the US Department of Energy at Los Alamos National Laboratory under contract DE-AV52-06NA25396. J. D. S. gratefully acknowledges the support of a Millikan Fellowship provided by Caltech.

REFERENCES

Baltz, E. A., Briot, C., Salati, P., Taillet, R., & Silk, J. 2000, Phys. Rev. D, 61, 023514
Baltz, E. A., Taylor, J. E., & Wai, L. L. 2007, ApJ, 659, L125
Barkana, R., & Loeb, A. 1999, ApJ, 523, 54
Belokurov, V., et al. 2007, ApJ, 654, 897
Benson, A. J., Lacey, C. G., Baugh, C. M., Cole, S., & Frenk, C. S. 2002, MNRAS, 333, 156
Bergstrom, L., & Hooper, D. 2006, Phys. Rev. D, 73, 063510
Bullock, J. S., & Johnston, K. V. 2007, in Island Universes: Structure and Evolution of Disk Galaxies, ed. R. de Jong (Dordrecht: Springer), 227
Bullock, J. S., Kravtsov, A. V., & Weinberg, D. H. 2000, ApJ, 539, 517
Calcaneo-Roldan, C., & Moore, B. 2000, Phys. Rev. D, 62, 123005
Chiu, W. A., Gnedin, N. Y., & Ostriker, J. P. 2001, ApJ, 563, 21
Cole, S., Aragon-Salamanca, A., Frenk, C. S., Navarro, J. F., & Zepf, S. E. 1994, MNRAS, 271, 781
Cortina, J. 2005, Ap&SS, 297, 245
Dekel, A., & Silk, J. 1986, ApJ, 303, 39
Diemand, J., Kuhlen, M., & Madau, P. 2007, ApJ, 657, 262
Diemand, J., Zemp, M., Moore, B., Stadel, J., & Carollo, M. 2005, MNRAS, 364, 665
Duquennoy, A., & Mayor, M. 1991, A&A, 248, 485
Evans, N. W., Ferrer, F., & Sarkar, S. 2004, Phys. Rev. D, 69, 123501
Fisher, R. T. 2004, ApJ, 600, 769
Gilmore, G., Wilkinson, M. I., Wyse, R. F. G., Kleyna, J. T., Koch, A., Evans, N. W., & Grebel, E. K. 2007, ApJ, 663, 948
Hanna, D. S., et al. 2002, Nucl. Instrum. Methods Phys. Res. A, 491, 126
Hofmann, W. 2003, in Proc. 28th Int. Cosmic Ray Conf. (Tsukuba), 2811
Hooper, D., & Dingus, B. L. 2004, Phys. Rev. D, 70, 113007
Hunter, S. D., et al. 1997, ApJ, 481, 205
Irwin, M. J., et al. 2007, ApJ, 656, L13
Kauffmann, G., White, S. D. M., & Guiderdoni, B. 1993, MNRAS, 264, 201
King, I. 1962, AJ, 67, 471
Klimentowski, J., Łokas, E. L., Kazantzidis, S., Prada, F., Mayer, L., & Mamon, G. A. 2007, MNRAS, 378, 353
Klypin, A., Kravtsov, A. V., Valenzuela, O., & Prada, F. 1999, ApJ, 522, 82
Koch, A., Wilkinson, M. I., Kleyna, J. T., Gilmore, G. F., Grebel, E. K., Mackey, A. D., Evans, N. W., & Wyse, R. F. G. 2007, ApJ, 657, 241
Koushiappas, S. M. 2006, Phys. Rev. Lett., 97, 191301
Koushiappas, S. M., Zentner, A. R., & Walker, T. P. 2004, Phys. Rev. D, 69, 043501
Łokas, E. L., Mamon, G. A., & Prada, F. 2005, MNRAS, 363, 918
Martin, N. F., Ibata, R. A., Chapman, S. C., Irwin, M., & Lewis, G. F. 2007, MNRAS, 380, 281
Mashchenko, S., Sills, A., & Couchman, H. M. P. 2006, ApJ, 640, 252
Mateo, M. L. 1998, ARA&A, 36, 435
Moore, B., Ghigna, S., Governato, F., Lake, G., Quinn, T., Stadel, J., & Tozzi, P. 1999, ApJ, 524, L19
Muñoz, R. R., et al. 2005, ApJ, 631, L137
Navarro, J. F., et al. 2004, MNRAS, 349, 1039
Nishimura, J., et al. 1980, ApJ, 238, 394
Olszewski, E., Pryor, C., & Armandroff, T. 1996, AJ, 111, 750
Peñarrubia, J., McConnachie, A., & Navarro, J. F. 2007, ApJ, 672, 904
Peñarrubia, J., Navarro, J. F., & McConnachie, A. W. 2008, ApJ, 673, 226
Piatek, S., & Pryor, C. 1995, AJ, 109, 1071
Pieri, L., Branchini, E., & Hofmann, S. 2005, Phys. Rev. Lett., 95, 211301
Profumo, S., & Kamionkowski, M. 2006, J. Cosmol. Astropart. Phys., 0603, 003
Ritz, S. M., et al. 2006, BAAS, 38, 1105
Sánchez-Conde, M. A., Prada, F., Łokas, E. L., Gómez, M. E., Wojtak, R., & Moles, M. 2007, Phys. Rev. D, 76, 123509
Simon, J. D., & Geha, M. 2007, ApJ, 670, 313
Sinnis, G. 2005, in AIP Conf. Proc. 745, High Energy Gamma-Ray Astronomy, ed. F. A. Aharonian, H. J. Völk, & D. Horns (New York: AIP), 234
Sollima, A., Beccari, G., Ferraro, F. R., Fusi Pecci, F., & Sarajedini, A. 2007, MNRAS, 380, 781
Somerville, R. S., & Primack, J. R. 1999, MNRAS, 310, 1087
Stoehr, F., White, S. D. M., Springel, V., Tormen, G., & Yoshida, N. 2003, MNRAS, 345, 1313
Strigari, L. E., Bullock, J. S., Kaplinghat, M., Diemand, J., Kuhlen, M., & Madau, P. 2007a, ApJ, 669, 676
Strigari, L. E., Koushiappas, S. M., Bullock, J. S., & Kaplinghat, M. 2007b, Phys. Rev. D, 75, 083526
Tasitsiomi, A., & Olinto, A. V. 2002, Phys. Rev. D, 66, 083006
van den Bosch, F. C., Tormen, G., & Giocoli, C. 2005, MNRAS, 359, 1029
Walker, M. G., Mateo, M., Olszewski, E. W., Bernstein, R. A., Wang, X., & Woodroofe, M. 2006, AJ, 131, 2114
Walker, M. G., Mateo, M., Olszewski, E. W., Gnedin, O. Y., Wang, X., Sen, B., & Woodroofe, M. 2007, ApJ, 667, L53
Walsh, S. M., Jerjen, H., & Willman, B. 2007, ApJ, 662, L83
Weekes, T. C., et al. 2002, Astropart. Phys., 17, 221
Westfall, K. B., Majewski, S. R., Ostheimer, J. C., Frinchaboy, P. M., Kunkel, W. E., Patterson, R. J., & Link, R. 2006, AJ, 131, 375
Willman, B., et al. 2005, ApJ, 626, L85
Yoshikoshi, T., et al. 1999, Astropart. Phys., 11, 267
Zentner, A. R., & Bullock, J. S. 2003, ApJ, 598, 49
Zucker, D. B., et al. 2006, ApJ, 650, L41